Cyclic mechanical behavior of Sn3.0Ag0.5Cu alloy under high temperature isothermal ageing

Benoit Dompierre, Véronique Aubin, Eric Charkaluk, Wilson Maia Filho, Michel Brizoux

Cyclic mechanical behaviour of Sn3.0Ag0.5Cu alloy under high temperature isothermal ageing

B. Dompierre[a,b,c,d,*], V. Aubin[a,b,c], E. Charkaluk[a,c], W.C. Maia Filho[d], M. Brizoux[d]

[a] *Univ Lille Nord de France, F-59000 Lille, France*
[b] *ECLille, LML, F-59650 Villeneuve d'Ascq, France*
[c] *CNRS, UMR 8107, F-59650 Villeneuve d'Ascq, France*
[d] *Engineering & Process Management, Thales Corporate Services SAS, 92366 Meudon, France*

For SnAgCu alloys, the results of previous studies suggest that high-temperature thermal ageing causes quick and significant deterioration of their mechanical properties. However, the acceleration law of thermal ageing and the relationship between thermal ageing and the cyclic mechanical behaviour remain unknown.

The aim of this study was to investigate the influence of isothermal ageing on the cyclic mechanical behaviour of Sn3.0Ag0.5Cu. First, ageing conditions were defined by taking into account the in-field operational conditions. Then, for all ageing conditions (75 °C, 125 °C and 150 °C up to 6500 h), the Vickers hardness was measured and the changes in this value were analysed during thermal ageing. At the same time, cross-polarised light microscopy observations on the same samples demonstrated the relation between the decrease in hardness and the changes in the microstructure for various samples. Finally, reversed mechanical cyclic tests were carried out at room temperature on specimens before and after ageing (125 °C, 500 h) in various conditions (strain rate/strain amplitude/dwell time).

1. Introduction

In the electronics industry, components are assembled on the printed circuit board using solder joints, which ensure the electric, thermal and mechanical connection between the board and the components. Before July 2006, most electronic products were assembled with eutectic SnPb alloy. Due to the July 2006 RoHS (Restriction of Hazardous Substances) directive, the mass market turned to lead-free processes for electronic assemblies. Most electronic manufacturers chose SnAgCu alloys.

Thermal ageing induces changes in the SnAgCu alloy's microstructure. The growth kinetics of the interface between the solder and substrates are well known [1–3]: for example, Siewert et al. [1] determined the equations and activation energies of the growth of intermetallic layers for four various lead-free alloys. In the bulk solder, two phenomena can be encountered. First, Wiese and Rzepka [4] observed the coalescence of intermetallic phases after thermal storage for 1500 h at 150 °C. Second, Telang et al. [5] demonstrated a grain size growth phenomenon for the Sn3.8Ag0.7Cu alloy. After thermal ageing for 200 h at 150 °C, the increase in the grain size was greater than 100%. Other studies [6,7] demonstrated that the same phenomenon is observed after thermal ageing at other high temperatures.

For thermal ageing of the interface layers, various studies have demonstrated the relation between the changes in the microstructure and in certain mechanical properties [8–11]. In these cases, ageing laws have been defined for various chemical compositions. Regarding the bulk alloy, Ma et al. [12] suggested that high-temperature thermal ageing causes a significant deterioration in mechanical properties such as hardness and yield stress after storage for hundreds of hours at 100 °C, but the relation between changes in the microstructure and in mechanical properties remains to be proved.

Moreover, until now, changes in bulk solder mechanical properties have been demonstrated using monotonic tests [12–16], which is a good but insufficient indicator of the influence of thermal ageing on the cyclic mechanical behaviour of SnAgCu alloys. The objective of the present study was to evaluate the influence of thermal ageing on the cyclic mechanical behaviour of SnAgCu alloys. This study is original in that it simultaneously analyses microstructure and cyclic mechanical behaviour changes.

This study was divided into three parts. First, the influence of thermal ageing on monotonic mechanical properties of the Sn3.0Ag0.5Cu alloy was evaluated. The Vickers hardness was

* Corresponding author at: Engineering & Process Management, Thales Corporate Services SAS, 18 Avenue du Maréchal Juin, 92366 Meudon la Foret, France.
Tel.: +33 1 70 28 23 92; Fax: +33 1 70 28 25 00.
E-mail address: benoit.dompierre@thalesgroup.com (B. Dompierre).

measured on as-received samples (specimens before ageing) and regularly during thermal ageing up to 6500 h at various temperatures making it possible to evaluate ageing kinetics and to define the thermal ageing conditions for the second phase of the study. Simultaneously, cross-polarised light microscopy was carried out to analyse the microstructure changes after thermal ageing. These results related the decrease in hardness to the changes in the microstructure. Finally, the effects of thermal ageing on mechanical properties were characterised using monotonic tensile tests and reversed cyclic tests. This paper is organised as follows. First, it presents the material studied and the experimental methodology. Then the results of hardness tests and polarised light microscopy observations are described and followed by the results of monotonic and cyclic tests. Finally, these results are summarised and the conclusions are presented.

2. Material

Many chemical compositions have been suggested to replace SnPb alloys. In large part because of their relatively low price and low melting point, SnAgCu alloys emerged and the majority of new brazing alloys are SnAgCu-based. For electronic products, Sn3.0Ag0.5Cu is a very widely used composition because it is a compromise between low melting point (near eutectic composition) and price (low Ag rate). For this reason, only the Sn3.0Ag0.5Cu composition was investigated in this study.

Because of the low melting point of SnAgCu alloys, around 220 °C, room temperature corresponds to 0.6 Tm (in Kelvin). Consequently, SnAgCu alloys present a time-dependent behaviour at room temperature and the effects of strain rate and stress relaxation cannot be neglected [17–22].

Regarding the microstructure, pure Sn presents three allotropic forms: α (diamond cubic) at 13 °C, β (body-centered tetragonal) between 13 °C and 161 °C and γ (orthorhombic) between 161 °C and 232 °C (Tm). In SnAgCu alloys, Sn accounts for more than 95% of the composition. The alloy's microstructure is therefore very similar to the microstructure of pure Sn: pure βSn dendrites surrounded by βSn. Ag can be found in Ag_3Sn needles or plates, while Cu_6Sn_5 precipitates are generally rod-like [23].

3. Experimental procedure

This section first presents the fabrication of specimens, then the hardness tests and the microstructural observations, and finally the reversed cyclic tests.

3.1. Fabrication of samples

For reproducibility purposes, all samples were extracted from the same batch of solder bars used for wave soldering. This ensures that the initial microstructure is the same for both the hardness and tensile tests. For hardness tests, the samples were extracted from solder bars by cutting with a band saw. The samples measured 10 mm × 10 mm × 30 mm, as shown in Fig. 1a. Band saw cutting generally warms the specimens. Great care was taken to achieve good lubrication of the solder bars while sawing so as to limit heating. In addition to this precaution, samples were prepared by polishing with the grit size ranging from 120 to 600 to remove the external layer of material, which could be affected by the cutting process.

Two main fabrication methods of the tensile specimens were compared: casting and machining. Casting problems have been encountered in some studies [23,24] in which polarised light microscopy demonstrated that only a few grains constituted the cross-section because the cooling rate was too low. A sample casting test demonstrated the same results. However, controlling grain size is crucial in this type of test. The grain size has to be homogeneous within all the specimens and small enough to consider the specimens as a representative elementary volume of the material. To ensure this condition, it is estimated that a specimen's cross-section must contain a minimum of 100 grains. Polarised light microscopy observations of the solder bars proved that the grain size in these bars was about 10 μm, which ensures thousands of grains in the specimen's cross-section. As the specimen obtained by casting did not encounter this condition, the specimens were extracted from solder bars from the batch used for hardness samples by high-pressure water cutting, as illustrated in Fig. 1b. Microstructure observations on the edges of the specimens showed that the impact of the water cutting on the microstructure was negligible. The specimen's dimensions and geometry are illustrated in Fig. 1b. The gauge part of the specimen was 10 mm in length, 10 mm in width and 10 mm in height.

Table 1
Ageing conditions.

Condition (°C)	Maximum ageing time tested (h)
75	6500
125	3000
150	1350

3.2. Isothermal ageing

For the former SnPb alloys, the influence of thermal ageing on the mechanical properties stabilises in a very short time. Miyazawa and Ariga [25] demonstrated that thermal storage for only 250 h at room temperature is enough to reach the thermally aged condition. For new SnAgCu alloys, previous studies seem to prove that there is a stabilisation state for thermal ageing for hundreds of hours at high temperature, but the relation with room temperature has not yet been clarified.

To evaluate this, bulk samples were thermally aged at three different temperatures (75 °C, 125 °C and 150 °C) up to 6500 h in order to characterise the isothermal acceleration of the phenomenon using hardness tests, as shown in Table 1. Each ageing condition was associated with at least one sample.

Thermal ageing at 125 °C was chosen in order to be coherent with the IPC9701A specification [26], which describes "use environments for surface mounted electronics". In this specification, the highest storage temperature for military aircraft is 125 °C. The second storage temperature, 150 °C, was chosen to create a higher acceleration phenomenon, which corresponds to the automotive (under the hood) maximum storage temperature. Finally, the third temperature, 75 °C, corresponds to a lower acceleration phenomenon and is half-way between room temperature (25 °C) and 125 °C.

3.3. Cross-polarised light observations

The βSn structure is body-centred tetragonal. Directions [1 0 0] and [0 1 0] present the same properties but the direction [0 0 1] differs, so that βSn has a birefringent behaviour. Using cross-polarised light, each grain orientation shows a different colour, so that the grains can be counted and measured.

Before the observation, one side of the samples was prepared using polishing paper with grit sizes ranging from 120 to 4000, then 3-, 1- and 0.25-μm Struers diamond pastes were used. For each observation, all grains within a circle of a defined area were identified. The results obtained were presented in a previous study [27]. Using ImageJ software, the area of each grain was measured. Then the mean diameter of the grain was calculated from the measured

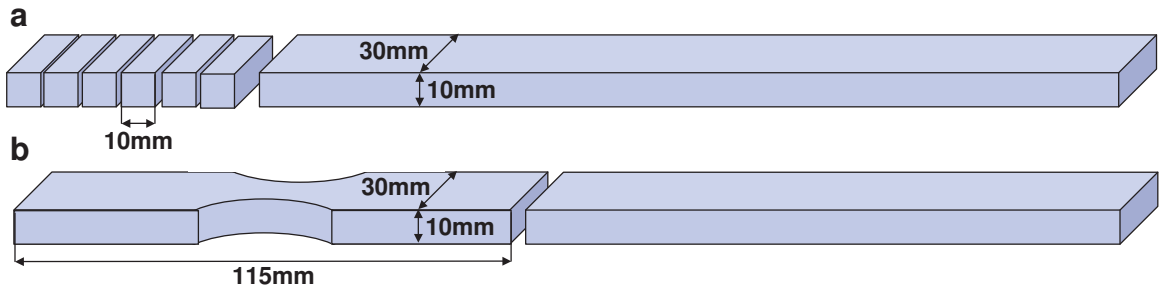

Fig. 1. (a) Fabrication of hardness test samples; (b) fabrication of tensile test specimens.

area assuming a circular grain. Finally, the grain size distribution was evaluated with these data.

While cooling the solder bar, the temperature drop is probably not the same in all locations. The highest difference in the cooling rate could be between the edge and the centre of the bars and can therefore influence grain size. Ingots were first observed before thermal ageing in order to study the possible influence of the testing site on the results. Two areas were analysed for comparison: the centre and the edge of the sample. Grain size was determined using cross-polarised microscopy observations as presented above. There was no significant difference between the centre of the sample and its edge. On these two locations, the mean grain size was about 4 μm for the as-received material.

Secondly, to establish whether a relation existed between the microstructure and thermal ageing, grain size distributions were estimated for various ageing conditions. For all samples, the distribution was fitted with a lognormal law.

3.4. Hardness tests

The results of hardness tests could be affected by the indented grain's crystal orientation. However, the bulk samples' mean grain size (d_m) was up to 10 μm (for the aged material) and the indenter size was about 1 mm^2. As the indenter size was much larger than the grain size, this ensured that a mean hardness value would be obtained.

The hardness tests were divided into two steps. First, in order to check whether the test location had an impact on the result, the scattering of the hardness was characterised over the entire surface. Consequently, 21 hardness tests were performed following a grid. As the relative standard deviation was 3%, it can be concluded that there is no significant influence of the test location on the results.

Secondly, the tests were performed with various ageing conditions. As described above, at room temperature, SnAgCu alloys present a time-dependent behaviour. Thus, to prevent scattering of the values measured, the duration of each test was carefully controlled. All tests were carried out at room temperature with a 30-N load applied for 10 s. For each sample, the hardness value was obtained by averaging at least nine values to reduce uncertainty. The results presented in the following section are the mean values of all the data measured in each test condition.

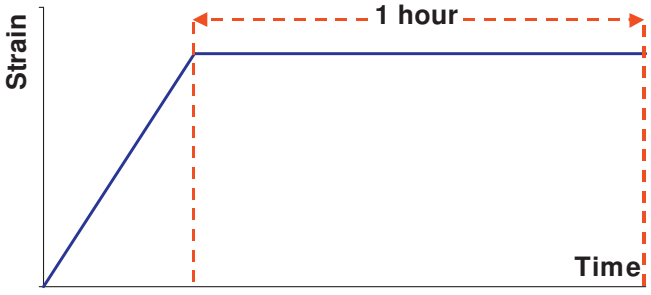

Fig. 2. Monotonic tensile test strain control.

3.5. Monotonic and reversed cyclic tests

All monotonic and cyclic tensile tests were carried out at room temperature on a 100-kN Instron servo-hydraulic tensile test machine. Strain was checked by means of an Instron contact extensometer with a 10-mm gauge length.

As previously specified, at room temperature, SnAgCu alloys present a time-dependent behaviour; the effects of the strain rate and stress relaxation have to be taken into account. Therefore, two types of tests were performed. First, monotonic tensile tests were carried out in order to determine the influence of the strain rate, the reproducibility between various specimens and relaxation characteristics. Fig. 2 presents the strain control shape for monotonic tensile tests.

Then reversed cyclic tests were carried out to analyse the changes of the mechanical behaviour during mechanical cycling for various strain amplitudes and strain rates. Fig. 3a presents the cyclic strain control without dwell time (triangular shape) and Fig. 3b presents the same cyclic control with dwell time (trapezoid shape).

All the parameters used for monotonic and cyclic tests are presented in Table 2. Strain amplitudes and strain rates were chosen

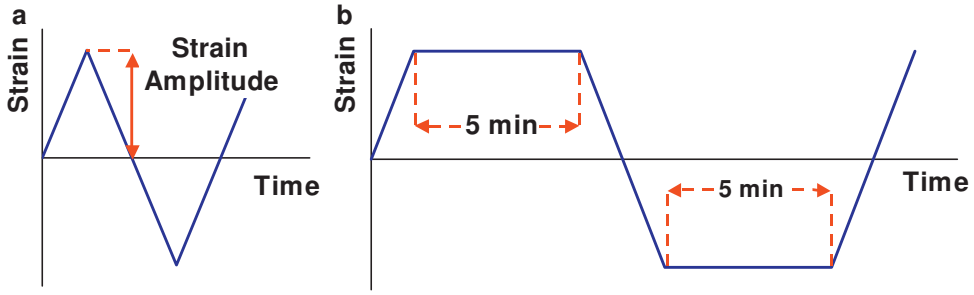

Fig. 3. (a) Reversed cyclic test strain control without dwell time. (b) Reversed cyclic test strain control with dwell time.

Table 2
Monotonic and cyclic testing conditions.

Monotonic tests	Strain rate (s^{-1})	2.10^{-3}	2.10^{-4}	2.10^{-5}
	Strain amplitude		0.2–2%	
	Dwell time		1 h	
Cyclic tests	Strain rate (s^{-1})	2.10^{-3}		2.10^{-4}
	Strain amplitude	0.2%	0.6%	1%
	Dwell time		0 or 5 min	

Table 3
Parameters of Eq. (1).

Parameter	Value
A	0.72
B	0.23
τ_0	3.31×10^{-8} h
E_a (activation energy)	0.77 eV
k (Boltzmann constant)	8.617×10^{-5} eV K^{-1}

to be coherent with the strain amplitudes that can be encountered in solder joints during thermal cycling tests. The dwell time for monotonic tests was chosen to ensure that stress stabilisation was reached. The dwell time for cyclic tests was chosen as a compromise between relaxation behaviour and test duration.

4. Results

4.1. Hardness tests

Fig. 4 shows the normalised values of hardness for four tested temperatures: 25 °C, 75 °C, 125 °C and 150 °C. In this figure, all the hardness values were divided by the initial value before ageing. This figure shows an approximately 30% decrease in hardness, followed by stabilisation for 125 °C and 150 °C. The stabilisation level obtained with samples aged at 125 °C was approximately 0.72, very close to the stabilisation level obtained with samples aged at 150 °C. These results suggest that the stabilisation level could be the same for both temperatures, which is consistent with the hypothesis of a single stabilisation state.

Regarding the results presented in Fig. 4, the decrease in hardness is related to ageing temperature and time. Eq. (1) was chosen to represent the changes observed. This equation corresponds first to an exponential decay to represent the time dependence with three parameters (A, B and τ) where the time parameter (τ) follows an Arrhenius law to represent the temperature dependence. The parameters of this equation were determined with data at 75 °C and 150 °C with a mean error of 1.9%. Data at 25 °C and 125 °C were then computed, and the comparison with experimental data gave a relative error of approximately 2.6% (Table 3).

$$H_v = A + Be^{-(t/\tau)} \quad \text{with} \quad \tau = \tau_0 e^{(E_a/kT)} \tag{1}$$

According to Fig. 4 and Eq. (1), above 125 °C, 95% of the stabilisation was reached after approximately 500 h. Complementary tests have to be made at 75 °C to confirm that there is only one steady state for all temperatures. If so, according to these results, thermal ageing for 500 h at 125 °C could be enough to reach the stabilised state for all temperatures. The ageing time at room temperature is highly inaccurate because of various uncertainties, one of which is activation energy (E_a). A 10% variation in E_a leads to a variation in stabilisation time at room temperature by a factor of 2. This means that the ageing time required before stabilisation at room temperature seems to be at least 20 years.

These results are in good agreement with the results of Ma et al. [12], who focused on the characterisation of the changes in monotonic mechanical properties using tensile tests on Sn4.0Ag0.5Cu. They demonstrated that the decrease in the Young modulus and the yield stress of this alloy seems to stabilise after thermal ageing for less than 500 h at 125 °C.

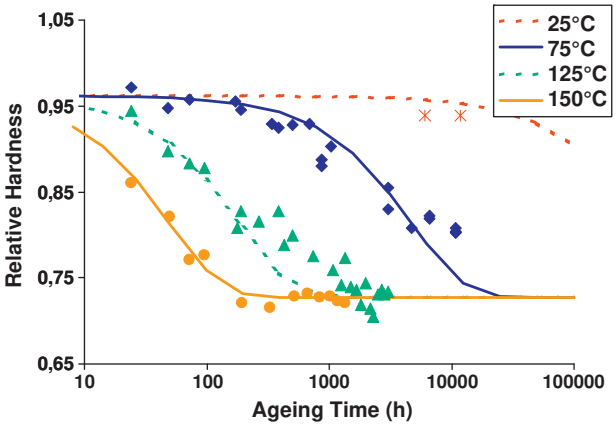

Fig. 4. Influence of ageing temperature and time on hardness with exponential fit [27].

4.2. Cross-polarised light observations

Fig. 5 compares the microstructures obtained initially and after thermal ageing at 125 °C for 384 h. The initial microstructure is very fine, with the grain size around 4 μm, whereas the aged microstructure presents very large grains. Comparing these two images demonstrates substantial grain growth.

Fig. 6 shows the distribution of grain sizes for Sn3.0Ag0.5Cu samples for the as-received condition. This distribution was esti-

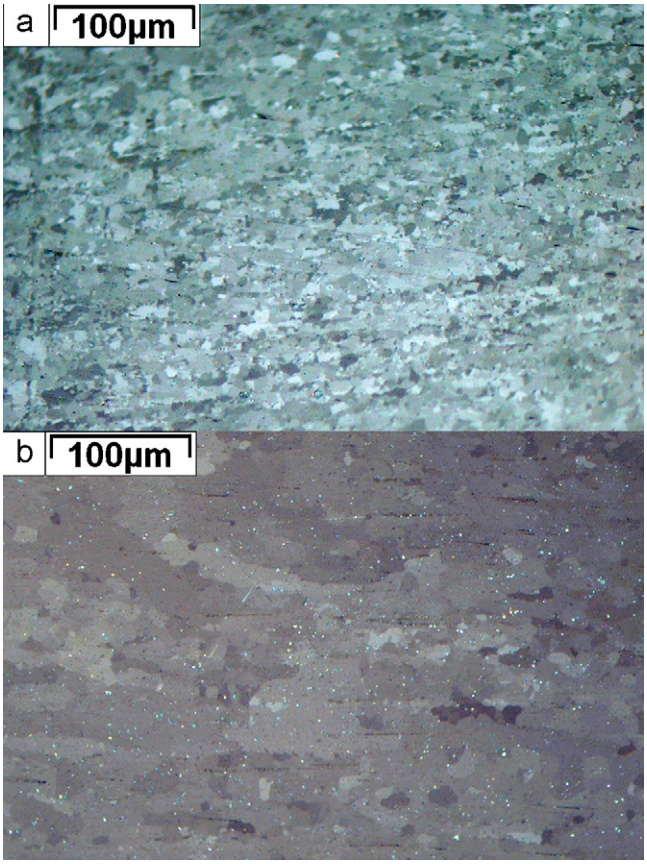

Fig. 5. (a) Initial microstructure and (b) microstructure after thermal ageing at 125 °C for 384 h.

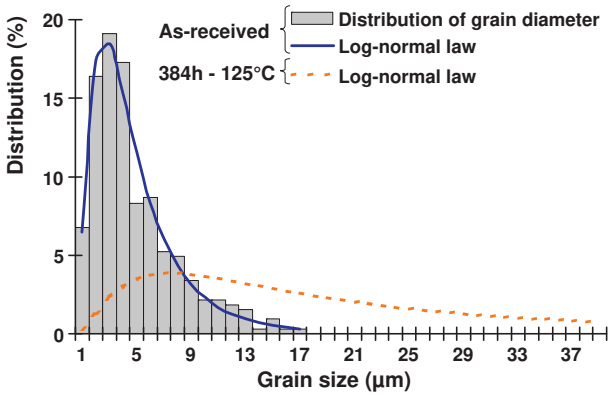

Fig. 6. Grain size distribution depending on the ageing condition.

mated with about 300 grains. Distributions corresponding to other ageing conditions are presented in a previous article [27]. From these results, two observations can be made: first, the mean grain size increased with ageing time; second, very large grains were more frequent when ageing time increased. Both observations can be made for the microstructures between 0 h, 72 h and 192 h, but no significant difference was observed between the microstructures after 192 h and 384 h. Differences between these two ageing conditions were probably so small that they were hidden by the uncertainties induced by the measurement method. For this reason, no additional observations were made after 384 h of thermal ageing at 125 °C.

4.3. *Influence of isothermal ageing on mechanical behaviour*

The objective of the following mechanical tests was to analyse the cyclic behaviour of the Sn3.0Ag0.5Cu alloy before and after ageing, when the stabilisation level has been reached. Two ageing conditions were chosen: specimens before ageing (as-received material) and specimens aged 500 h at 125 °C (aged material).

Fig. 7a shows the mechanical responses to monotonic tensile tests at two strain rates (2.10^{-3} s^{-1} and 2.10^{-4} s^{-1}) with specimens before and after ageing. Each condition was tested at least three times. Good reproducibility between specimens was observed so that only one test per condition during cyclic test analysis was necessary. Fig. 7b shows the relaxation behaviour during the dwell time. Stabilisation was reached about 1 h after dwell time began.

The influence of the strain rate on the maximum stress is shown in Fig. 8, in which the influence of the strain rate is characterised by an 18–22% decrease in the maximum stress for a decrease in the strain rate by a factor of 10. These results are in good agreement with Wang et al. [28], who determined that for two strain rates, 2.10^{-3} s^{-1} and 2.10^{-5} s^{-1}, the yield stress differs by 30%. In the present study, this was valid before and after ageing.

The influence of thermal ageing can be seen in Fig. 8. For each strain rate, the maximum stress was 35–40% lower for the aged condition than for as-received specimens. Moreover, for all the loading conditions considered, after the dwell time, the specimens reached the same stabilisation level, depending only on the ageing condition (as-received or aged material). The stress after the dwell time obtained on aged material was half the stress of the as-received material.

Fig. 9a shows the behaviour of the material during stress relaxation. The data were normalised as follows: maximum stress, the value referred to as "start of dwell time" in Fig. 7b, was converted to "1" and the stress value after dwell time, referred as "stabilisation level" in Fig. 7b, was converted to "0". Fig. 9a illustrates

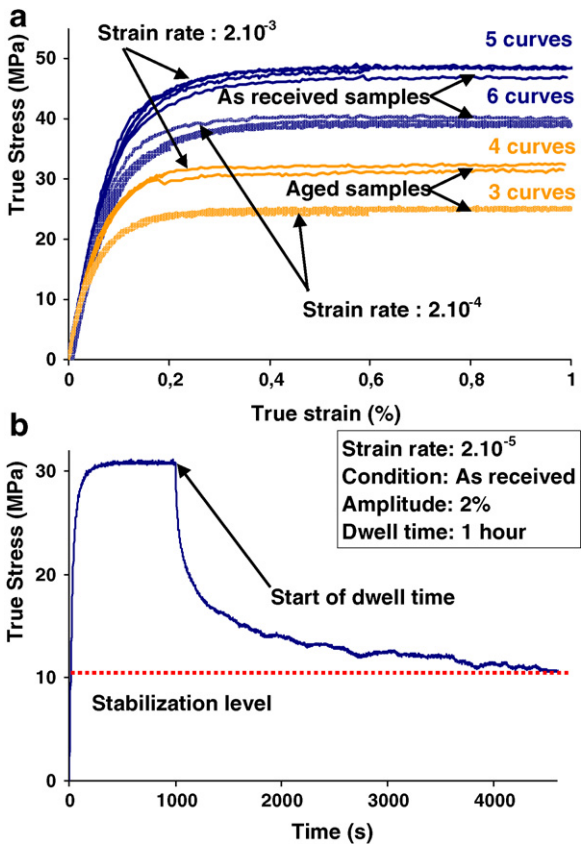

Fig. 7. (a) Strain–stress curves in various loading conditions. (b) Example of stress relaxation during dwell time.

that aged and as-received materials presented similar stress relaxation behaviours, which suggests that the viscous behaviour is not modified by thermal ageing. Fig. 9b shows that more than 90% of the stress relaxation was achieved before 30 min. The relaxation time depends on the strain rate and was the same for as-received and aged specimens. The higher the strain rate was, the faster the relaxation was, as shown in Fig. 9b.

Fig. 10 shows softening curves without normalisation for as-received and aged specimens under various conditions. These curves present a softening time, which leads to stabilisation or a quasi-stabilisation of the stress amplitude. These results are quite similar to those reported by Kanchanomai et al. [29], who obtained a softening cyclic behaviour for four lead-free alloys, including Sn3.0Ag0.5Cu.

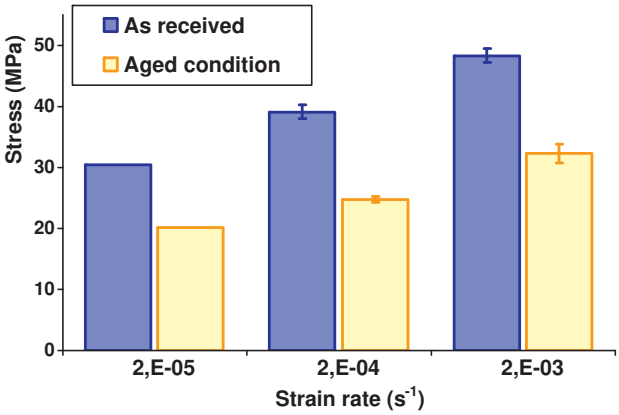

Fig. 8. Influence of the strain rate on the stress obtained when strain = 1%.

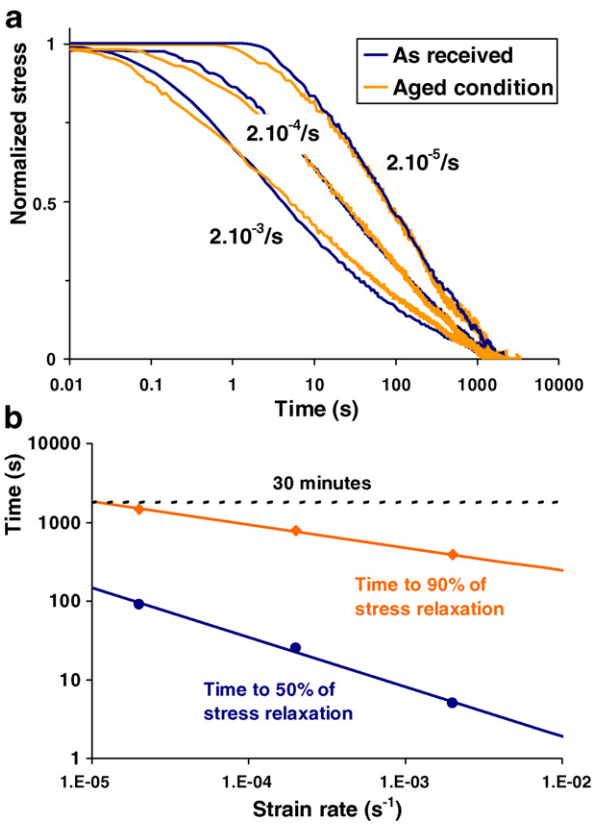

Fig. 9. (a) Influence of strain rate on relaxation behaviour. (b) Influence of strain rate on relaxation time.

Two points should be underlined:

- As for monotonic tests, thermal ageing induced a nearly 40% drop in stress amplitude. This direct comparison between as-received and aged conditions is possible because a good reproducibility between specimens had been observed previously;
- Even if the results of tests with and without the dwell time are not exactly the same, no clear effect of dwell time on stress amplitude was found. For a test condition, the dotted line (reversed cyclic test with dwell time) can be above or below the solid line (reversed cyclic tests without dwell time) corresponding to the same test condition.

In the following figures, all the data were normalised to make the comparison clearer. For each curve, all data were divided by the

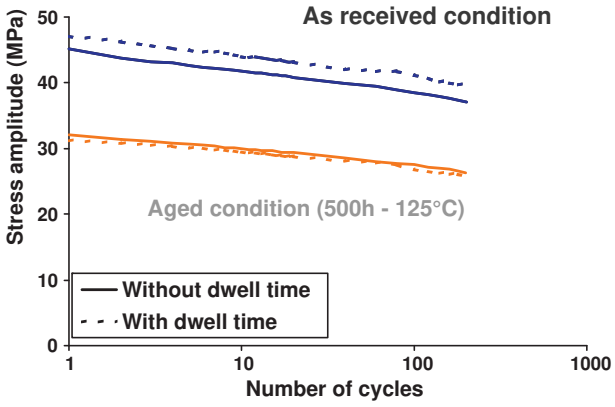

Fig. 10. Cyclic softening curve – strain amplitude = 1% – strain rate = 2.10^{-3} s^{-1}.

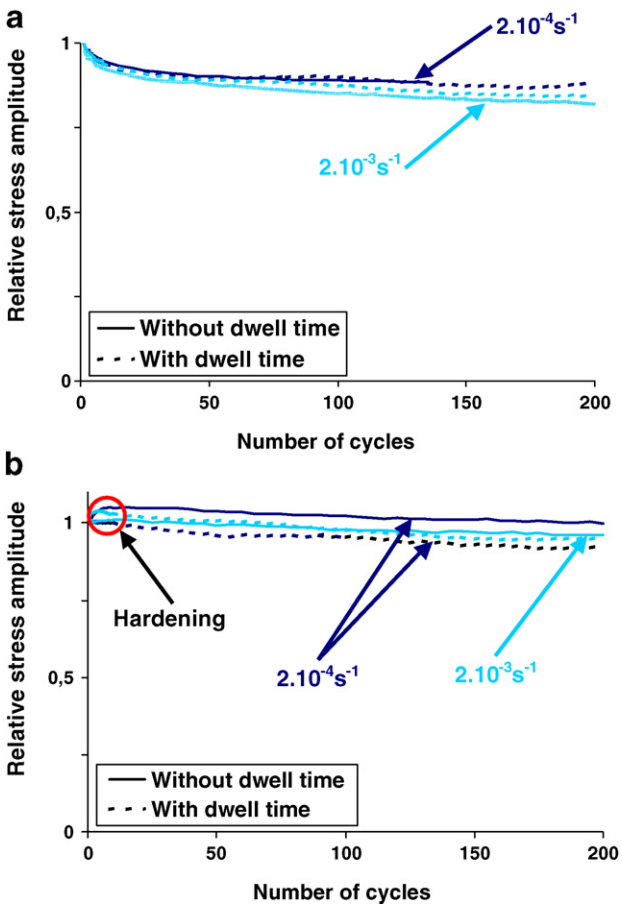

Fig. 11. As-received specimens – cyclic hardening/softening curve with a strain amplitude of (a) 1% and (b) 0.2%.

stress amplitude value of the first cycle, so that the first value for each curve was "1".

Fig. 11 shows the cyclic hardening/softening on as-received specimens. For the strain amplitude of 0.2%, shown in Fig. 11b, the first five cycles resulted in the material hardening (first stage) followed by softening (second stage), which finally provided quasi-stabilisation. The same general behaviour can be seen in Fig. 11a, for the strain amplitude of 1%. However, in that case, the hardening phase did not exist. It can also be noted that the stabilised stress amplitude at a strain amplitude of 1% was lower than the strain amplitude at 0.2%. For aged specimens, the cyclic behaviour was only a softening behaviour, as shown in Fig. 10. After 200 cycles, the drop in stress amplitude was the same as the as-received specimens (about 20%).

4.4. Discussion

In this study, hardness tests, monotonic tensile tests and cyclic reversed tests were carried out on the Sn3.0Ag0.5Cu alloy. In all these tests, the material was highly deformed (1% for tensile tests and more than 10% for hardness tests). The as-received and the aged materials differed in terms of hardness by about 30%. In tensile tests, maximum stress and the stress reached after relaxation differed by 40% and 50%, respectively. These deviations were also observed during cyclic tests with or without dwell time. These similarities are not surprising given that both tests measure the elastoplastic behaviour of the material and it is well known that hardness and yield stress are often linked by empirical relationships [30], which is even more accurate when the behaviour is perfectly plastic, as is Sn3.0Ag0.5Cu.

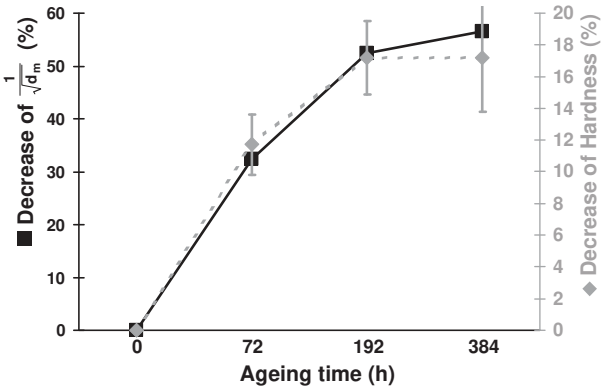

Fig. 12. Decrease in hardness and increase in grain size over time at 125 °C.

The results also show that thermal ageing induces an increase in grain size and a decrease in hardness. For metallic materials, the yield stress is often related to the grain size through the Hall–Petch law [31], presented in Eq. (2). Fig. 12 represents the decrease in the hardness value and the grain size growth over time during isothermal ageing at 125 °C. The grain growth is correlated to the decrease of $1/\sqrt{d}$. The hardness and the grain size follow analogous variations according to time and temperature, which confirms that grain growth and changes in mechanical properties may be related. This type of relationship is generally observed in metallic materials [32].

$$\sigma_y = \sigma_0 + \frac{k}{\sqrt{d}} \tag{2}$$

5. Conclusions

The aim of this paper was to improve the understanding of the microstructural and mechanical changes during thermal ageing of the Sn3.0Ag0.5Cu alloy and their impact on the cyclic behaviour of the alloy.

Assessing ageing through hardness tests and polarised light microscopy demonstrated that thermal ageing induces an increase in grain size and a decrease in hardness. These two phenomena are strongly related through a Hall–Petch-type relationship. Ageing ends (95% achieved) after about 500 h at 125 °C and this ageing condition is equivalent to more than 20 years at room temperature. Therefore, for systems intended to have a long lifespan, it appears that ageing may occur before or during the operational phase and evaluating the influence of thermal ageing on the reliability of electronic assemblies is required.

The mechanical behaviour of Sn3.0Ag0.5Cu was evaluated by monotonic and cyclic tensile tests on as-received and aged materials. The results of these tests show common points between these two materials. First, the influence of the strain rate is a well-known phenomenon for Sn3.0Ag0.5Cu and remains the same after thermal ageing for 500 h at 125 °C. Then the relaxation behaviour remains the same, and depends only on the strain rate. Finally, the softening behaviour seems to be the same with a 20% decrease in stress amplitude after 200 cycles with or without dwell time. However, major differences can be noted between as-received and aged materials. First, the stress amplitude during monotonic or cyclic tests is about 40% lower after thermal ageing. Secondly, after dwell time, stress is halved in specimens after compared to before isothermal ageing.

All these observations lead to the conclusion that thermal ageing must be fully understood in the reliability analysis of solder joints on electronic assemblies. Complementary studies have to be conducted first in solder joint scaled specimens to validate the influence of thermal ageing at the joint scale and then on the assembled board. These studies are in progress [16,27].

References

[1] T.A. Siewert, J.C. Madeni, S. Liu, Proceedings of the APEX Conference on Electronics Manufacturing, Anaheim, CA, 2003.
[2] S. Choi, T. Bieler, J. Lucas, K. Subramanian, Journal of Electronic Materials 28 (1999) 1209–1215.
[3] Y. Tian, C. Wang, W. Zhou, Acta Metallurgica Sinica (English Letters) 19 (2006) 301–306.
[4] S. Wiese, S. Rzepka, Microelectronics Reliability 44 (2004) 1893–1900.
[5] A. Telang, T. Bieler, J. Lucas, K. Subramanian, L. Lehman, Y. Xing, E. Cotts, Journal of Electronic Materials 33 (2004) 1412–1423.
[6] L. Xu, J. Pang, Proceedings of the 56th Electronic Components and Technology Conference (ECTC 2006), 2006, pp. 275–282.
[7] B. Dompierre, V. Aubin, E. Charkaluk, W. Maia Filho, M. Brizoux, Proceedings of the 10th International Conference on Thermal Mechanical and Multi-Physics Simulation and Experiments in Microelectronics and Micro-Systems (EuroSimE), Delft, Nederland, 2009, pp. 342–347.
[8] R. Zhang, F. Guo, J. Liu, H. Shen, F. Tai, Journal of Electronic Materials 38 (2009) 241–251.
[9] I. Anderson, J. Harringa, Journal of Electronic Materials 33 (2004) 1485–1496.
[10] L. Xu, J. Pang, Journal of Electronic Materials 35 (2006) 2107–2115.
[11] H. Lu, H. Balkan, K. Ng, Journal of Materials Science: Materials in Electronics 17 (2006) 171–178.
[12] H. Ma, Y. Zhang, Z. Cai, J.C. Suhling, P. Lall, M.J. Bozack, Proceedings of the 9th International Conference on Thermal Mechanical and Multi-Physics Simulation and Experiments in Microelectronics and Micro-Systems (EuroSimE), Freiburg, Germany, 2008, pp. 335–346.
[13] S. Wiese, M. Roellig, K. Wolter, Proceedings of the 55th Electronic Components and Technology Conference (ECTC 2005), vol. 2, 2005, pp. 1272–1281.
[14] I. Anderson, J. Harringa, Journal of Electronic Materials 35 (2006) 94–106.
[15] C. Wei, Y. Liu, Z. Gao, J. Wan, C. Ma, Journal of Electronic Materials 38 (2009) 345–350.
[16] B. Dompierre, V. Aubin, E. Charkaluk, W. Maia Filho, M. Brizoux, Procedia Engineering 2 (2010) 1477–1486.
[17] K.S. Kim, S.H. Huh, K. Suganuma, Materials Science and Engineering A 333 (2002) 106–114.
[18] E.S.W. Poh, W.H. Zhu, X.R. Zhang, C.K. Wang, A.Y.S. Sun, H.B. Tan, Proceedings of the 9th International Conference on Thermal, Mechanical and Multi-Physics Simulation and Experiments in Microelectronics and Micro-Systems (EuroSimE), 2008, pp. 627–634.
[19] Z. Jun, C. GuoZhong, L. Yong, L. LiHua, H. WeiNa, Proceedings of the 8th International Conference on Thermal, Mechanical and Multi-Physics Simulation Experiments in Microelectronics and Micro-Systems (EuroSimE), 2007, pp. 1–7.
[20] M. Pei, J. Qu, Proceedings of the International Symposium on Advanced Packaging Materials: Processes, Properties and Interfaces, 2005, pp. 45–49.
[21] N. Bai, X. Chen, International Journal of Plasticity 25 (2009) 2181–2203.
[22] R. Metasch, J. Boareto, M. Roellig, S. Wiese, K. Wolter, Proceedings of the 10th International Conference on Thermal, Mechanical and Multi-Physics Simulation and Experiments in Microelectronics and Micro-Systems (EuroSimE), 2009, pp. 322–329.
[23] S. Park, R. Dhakal, L. Lehman, E. Cotts, Components and Packaging Technologies 30 (2007) 178–185.
[24] M. Matin, W. Vellinga, M. Geers, Materials Science and Engineering A 431 (2006) 166–174.
[25] Y. Miyazawa, T. Ariga, Proceedings of the First International Symposium On Environmentally Conscious Design and Inverse Manufacturing (EcoDesign'99), Tokyo, Japan, 1999, pp. 616–619.
[26] IPC (2006).
[27] B. Dompierre, W. Maia Filho, M. Brizoux, V. Aubin, E. Charkaluk, Microelectronics Reliability 50 (2010) 1661–1665.
[28] Q. Wang, L. Liang, Y. Liu, Proceedings of the 7th International Conference on Electronic Packaging Technology (ICEPT'06), Shanghai, 2006, pp. 1–4.
[29] C. Kanchanomai, Y. Miyashita, Y. Mutoh, Journal of Electronic Materials 31 (2002) 456–465.
[30] A.C. Fischer-Cripps, Nanoindentation, Second edition, Springer, 2004.
[31] N. Hansen, Scripta Materialia 51 (2004) 801–806.
[32] B.J. Moniz, Metallurgy, Fourth edition, American Technical Publishers, Inc., 2007.